

Nanostructured tetragonal crystal NdVO₄ for the detection of liquefied petroleum gasD. R. Kamble¹, S. V. Bangale^{2*}, S. R. Bamane³¹Department of Chemistry, Shankarrao Mohite Mahavidyalay, Akluj 413 101,
PAH University of Solapur, Maharashtra, India²Department of Chemistry, G. M. Vedak College of Science, Tala 402 111, University of Mumbai, Maharashtra, India³Sushila Shankarrao Mahavidyalay, Khandala, Dist. Satara, Shivaji University Kolhapur Maharashtra, India

*sachinbangale98@gmail.com

DOI 10.17586/2220-8054-2021-12-2-199-209

Semiconductive nanometer-sized NdVO₄ was synthesized by a solution combustion reaction of Nd(NO₃)₃·6H₂O, V(NO₃)₃ and urea as a fuel. The process was a convenient, environment friendly, inexpensive and efficient preparation method for the NdVO₄ nanomaterial. Effects of the 800 °C calcining temperature on the phase constituents was characterized by TG-DTA, X-ray diffraction (XRD), which was used to confirm the material's structure. The as-prepared samples were further characterized by scanning electron microscopy (SEM) equipped with energy-dispersive X-ray spectroscopy (EDX), and transmission electron microscopy (TEM), to depict the crystallite microstructure. Conductance responses of the nanocrystalline NdVO₄ thick film were measured by exposing the film to reducing gases like acetone, ethanol, ammonia (NH₃), and liquefied petroleum gas (LPG). It was found that the sensors exhibited various sensing responses to these gases at different operating temperatures. Furthermore, the sensor exhibited a fast response and a good recovery. The results demonstrated that NdVO₄ can be used as a new type of gas-sensing material which has a high sensitivity and good selectivity to Liquefied petroleum gas (LPG).

Keywords: solution combustion reaction, Synthesis, NdVO₄ nanoparticles, gas sensor.

Received: 1 February 2021

Revised: 8 March 2021

Final revision: 15 March 2021

1. Introduction

With the growing attention to environmental problems and the increase of standard of living, there are imperative needs for solid state gas sensors with high sensitivity and excellent selectivity, in air quality monitoring. LPG is widely used as a fuel for industrial and domestic purposes. It is one of the potentially proved hazardous gases due to explosive accidents when accidentally leaked. It is therefore important to develop a good sensor for the detection of LPG. Gas sensors based on metal oxide semiconductors generally involve a catalytic reaction of the gas or vapor on the surface of sensor. Gas sensors prepared with metal oxides have been used as detectors for some combustible and toxic gases. Rare earth and transition metal oxides are very important materials for use in the advanced technologies such as solid oxide fuel cells, as catalysts, as materials for electrodes and for chemical sensors because of their functional properties. Rare earth metal oxides are very promising for monitoring the environment due to their high sensitivities and appropriate selectivity. Simple metal oxides such as SnO₂, WO₃, ZnFe₂O₄, ZrCo₂O₄, MgFe₂O₄, and TiO₂ are well known for their high sensitivity to changes in the surrounding gas atmosphere, as can be shown by the growing number of papers [1–7]. Gas sensors based on rare earth mixed oxides materials reported mainly focused on detecting ethanol or NO_x. For example: Aono et al. have carried out more systemic research about SmFeO₃ and REFeO₃ (Re = La, Nd, Sm, Gd, and Dy) detecting NO₂ [8, 9]. Vanadium doped tin dioxides exhibit a higher response towards SO₂ gas, because of their redox activity for SO₂ oxidation to SO₃ [10]. Catalytic additives, such as CuO [11], MoO₃ [12, 13] and Fe₂O₃ [14] are known to lower sensor temperature and increase gas response. In spite of so many excellent results, experimental studies combining electrical with spectroscopic measurements to elucidate sensing mechanisms are still rather limited [15].

The mixed metal oxide materials are well known for their good stability, low cost and catalytic activity. Mixed metal oxides such as Co, Zn, and Ni, along with rare earths like La and Ce, are reported to be synthesized by sol-gel auto combustion method [16]. For these nanomaterials, the size of the particles becomes smaller as the ratio of total surface area to volume increases, which can affect many physical, chemical, mechanical, optical, and magnetic properties of these materials. Vanadates are particularly suitable hosts for luminescent applications. Among the rare earth vanadates, NdVO₄ belongs to zircon structure with space group I4₁/amd. It crystallizes in the tetragonal structure, composed of slightly distorted VO₄³⁻ tetrahedral and rare earth ion Nd³⁺ between the neighboring tetrahedral. Each Nd³⁺ ion is surrounded by eight oxygen ions. NdVO₄ nanoparticles were prepared by wet chemical methods. Au et al. synthesized NdVO₄ particles using the citrate method, and their catalytic properties were studied by oxidative

dehydrogenation of propane. The effects of Eu^{3+} doping on morphology and fluorescent properties of neodymium vanadate nanorod-arrays were studied [17,18]. Fan et al. synthesized single crystalline tetragonal nanorods of NdVO_4 through hydrothermal method and explained the growth mechanism [19]. The synthesis of NdVO_4 nanoparticles by a microwave method and the photocatalytic activity of NdVO_4 for degradation of methylene blue were studied [20]. The magnetic susceptibility of single crystal NdVO_4 was assessed at temperatures ranging from 10 mK to 300 K [21]. Magnetic properties of NdVO_4 particles through temperature dependence magnetic field [22]. NdVO_4 nanoparticles have many unique photoelectric properties which could be suggested to use extensively into the fields of X-ray imaging, biological labeling, solid state laser and displays. High ordered NdVO_4 nanotubes were fabricated using porous anodized aluminum oxide template (AAO) combined with sol-gel method [23].

Herein, we prepared NdVO_4 nanopowder by this simple solution combustion reaction. One of our aims is to develop a general synthesis method and explore the gas sensing properties of the NdVO_4 nanopowder obtained. We found that the process is a convenient, environment friendly, inexpensive and efficient for preparation of NdVO_4 nanomaterial with the grain size of about 15 – 35 nm. Furthermore, the NdVO_4 obtained possessed excellent gas-sensing responses to reducing gas. In the present paper we report the development of thick film NdVO_4 LPG sensors.

2. Experimental

2.1. Sample preparation and characterization

In this study polycrystalline NdVO_4 powder was prepared via the combustion route using urea as the fuel. The materials used as precursors were $\text{Nd}(\text{NO}_3)_3 \cdot 6\text{H}_2\text{O}$, $\text{V}(\text{NO}_3)_3 \cdot 6\text{H}_2\text{O}$ and urea (Nuclear band). Urea possesses a high heat of combustion. It is an organic fuel and provides a platform for redox reactions during the course of combustion. Initially the Neodymium Nitrate, Vanadium Nitrate and urea are combined in a 1:1:4 stoichiometric ratio and dissolved in a 250 ml beaker then slowly stirred using a glass rod, providing a clear solution. Solution formed was evaporated on hot plate in temperature range 70 to 80 °C gives thick gel. The gel was kept on a hot plate for auto combustion and heated in the temperature range 180 to 190 °C. The nanocrystalline NdVO_4 powder was formed within 40 – 50 minute. And then sintered at about 800 °C for about 4 hours then we obtain a yellow shining powder of nanocrystalline NdVO_4 .

Neodymium Vanadate oxide powder was ground in an agate mortar and pestle to ensure sufficiently fine particle size. The fine powder was calcined at 800 °C for 24 h in air and re-ground. The thixotropic paste [24, 25] was formulated by mixing the resulting NdVO_4 fine powder with a solution of ethyl cellulose (a temporary binder) in a mixture of organic solvents such as butyl carbitol acetate, and turpineol. The ratio of inorganic and organic path was kept as 75:25 in formulating the paste. The paste was then used to prepare thick films. The thixotropic paste was screen printed on a glass substrate in desired patterns. The films prepared were fired at 500 °C for 24 h.

2.2. Characterization techniques

The synthesized NdVO_4 nanoparticles are characterized using Thermogravimetric Differential Thermal Analyzer (TG-DTA, PERKIN ELMER, USA, and Diamond TG/DTA). The crystallinity and crystal phase were characterized by X-ray diffraction (XRD, Bruker, D8 – advanced diffractometer) pattern measured with $\text{Cu-K}\alpha$ Radiation ($\lambda = 1.5406 \text{ \AA}$) in the range of 20 – 60 °. The morphology and composition of the synthesized NdVO_4 nanoparticles were examined by scanning electron microscopy (SEM, JEOL, JSM-6360), SEM coupled energy dispersive X-ray spectroscopy (EDX, Bruker, XFlash 6130). The exact morphological structure and size of NdVO_4 nanoparticles were examined by Transmission Electron Microscopy (TEM) with Selected Area Electron Diffraction (SEAD) by using a Philips, CM 200 with an accelerating voltage of 200 kV. The Fourier Transform Infrared (FT-IR) spectrum was recorded by JASCO 4100 in the range of 4000 – 400 cm^{-1} . The optical properties were measured by UV-Visible Spectrophotometer (JASCO-Spectrophotometer, V-770) and DRS is obtained at the scanning range of 200 – 800 nm.

2.3. Fabrication and analysis of gas sensors

The sensing performance of the sensors was examined using a static gas-sensing system. There were electrical feeds through the base plate. The heating was constant on the base plate to heat the sample under test up to required operating temperatures. The current passing through the heating element was monitored using a relay with adjustable ON/OFF time intervals. A Cr–Al thermocouple was used to sense the operating temperature of the sensors. The output of the thermocouple was connected to digital temperature indicators. A gas inlet valve was fitted at one port of the base plate. The required gas concentration inside the static system was achieved by injecting a known volume of test gas using a gas-injecting syringe. A constant voltage was applied to the sensors, and current was measured by a digital Pico-ammeter. Air was allowed to pass into the glass dome after every gases exposure cycle in shown Fig. 1.

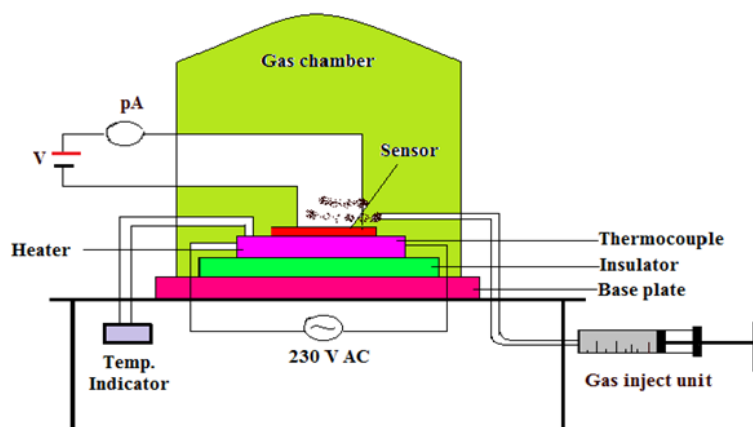


FIG. 1. Block diagram of static gas sensing setup

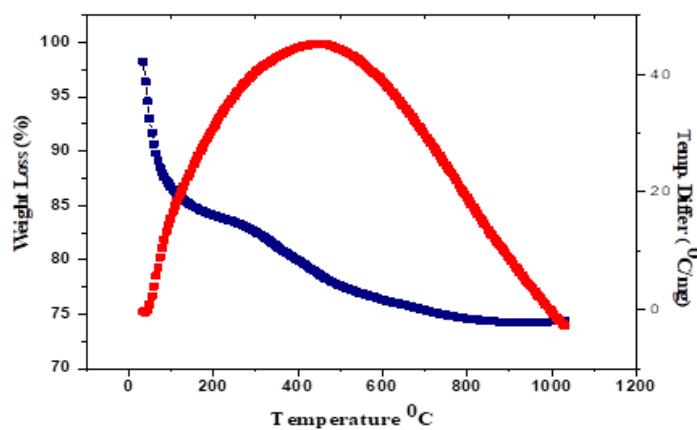
3. Result and discussion

3.1. TG-DTA analysis

When reactants were heated at 180 °C the reaction proceeded by the mechanism indicated in Eq. (1.1) to give the final product NdVO₄.



The TG curve recorded for thermal decomposition of NdVO₄ is shown in Fig. 2. The curve indicates that the slight weight loss in NdVO₄ powder was due to little loss of moisture, carbon dioxide and nitrogen gas. The DTA curve of NdVO₄ recorded in static air and shown in Fig. 2. The curve shows that NdVO₄ did not decompose, but weight loss was due to dehydrogenation, decarboxylation and denitration and yield final product at 800 °C. This weight change in the synthesized powder was stable from the beginning.

FIG. 2. TG-DTA curve of mixed precursor NdVO₄

3.2. XRD analysis

The synthesis of NdVO₄ was confirmed by characteristic peaks observed in the XRD pattern as shown in Fig. 2. Such a powder XRD was carried out using monochromatic CuK α -1 radiation (wavelength = 1.5406 Å) operating at a voltage of 40 KV and a current of 40 mA in the angular range 2 θ of 20 – 60 degree. XRD analysis showed a series of diffraction peaks at 24.18, 32.84, 34.60, 39.39, 48.40 and 49.78° corresponding to (200), (112), (220), (301), (312) and (400) crystal planes of tetragonal NdVO₄ nanostructures (JCPDS No. 82-1971). The sharp XRD peaks exposed for synthesized NdVO₄ nanoparticles are good crystalline in nature and show tetragonal structure with lattice constants

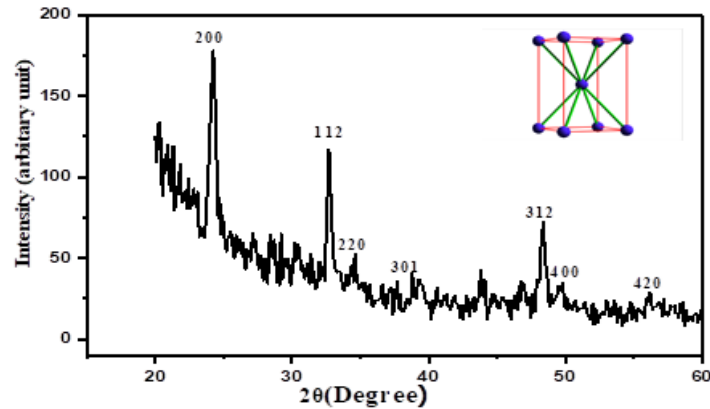


FIG. 3. XRD pattern of calcined mixed precursor NdVO_4 at $800\text{ }^\circ\text{C}$

$a = b = 7.32\text{ \AA}$ and $c = 6.42\text{ \AA}$ which are in good agreement with standard values of $a = b = 7.33\text{ \AA}$ and $c = 6.43\text{ \AA}$ which is shown in Fig. 3.

$$K = \frac{0.9\lambda}{\beta \cos \theta}. \quad (2)$$

Crystallite size was calculated by using Debye–Scherrer’s Formula by using Eq. (2). It was found to be 27 nm.

3.3. FT-IR analysis

The functional groups of synthesized NdVO_4 nanoparticles analyzed by FT-IR spectra recorded in the region of $400 - 4000\text{ cm}^{-1}$ are shown in Fig. 4. A sharp peak at 446 cm^{-1} is due to stretching vibrations of VO_4 [26]. A broad peak at 798 cm^{-1} is attributed to V–O vibrations of VO_4 [27]. A broad peak at 3433 cm^{-1} is easily assigned to O–H stretching vibrations from adsorbed water on the surface of NdVO_4 [28].

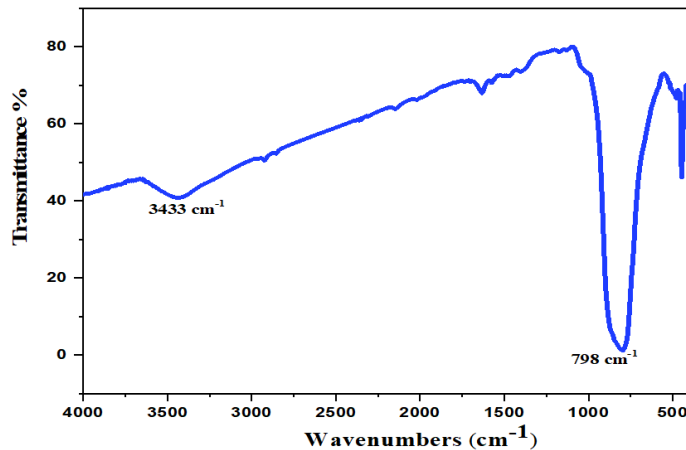


FIG. 4. FTIR spectra of synthesized NdVO_4 nanoparticles

3.4. SEM analysis

Morphologies and sizes of synthesized NdVO_4 nanoparticles were examined by SEM techniques. These micrographs reveal micro structural aspects related to size and morphology of particles or grains and pores at the sintering temperature $800\text{ }^\circ\text{C}$. The sample showed micro structural aspects of initial stage of the solid state sintering (SSS) process. Most of the NdVO_4 nanoparticles were linked to adjacent particles forming a neck between particles and interconnected network of tortuous porous channels (open porosity) in Fig. 5(a, b, c, d). It was seen that the NdVO_4 powder has smooth morphologies and developed grain size. A random distribution and agglomeration of particles was observed. The average particle size is 40 to 80 nm.

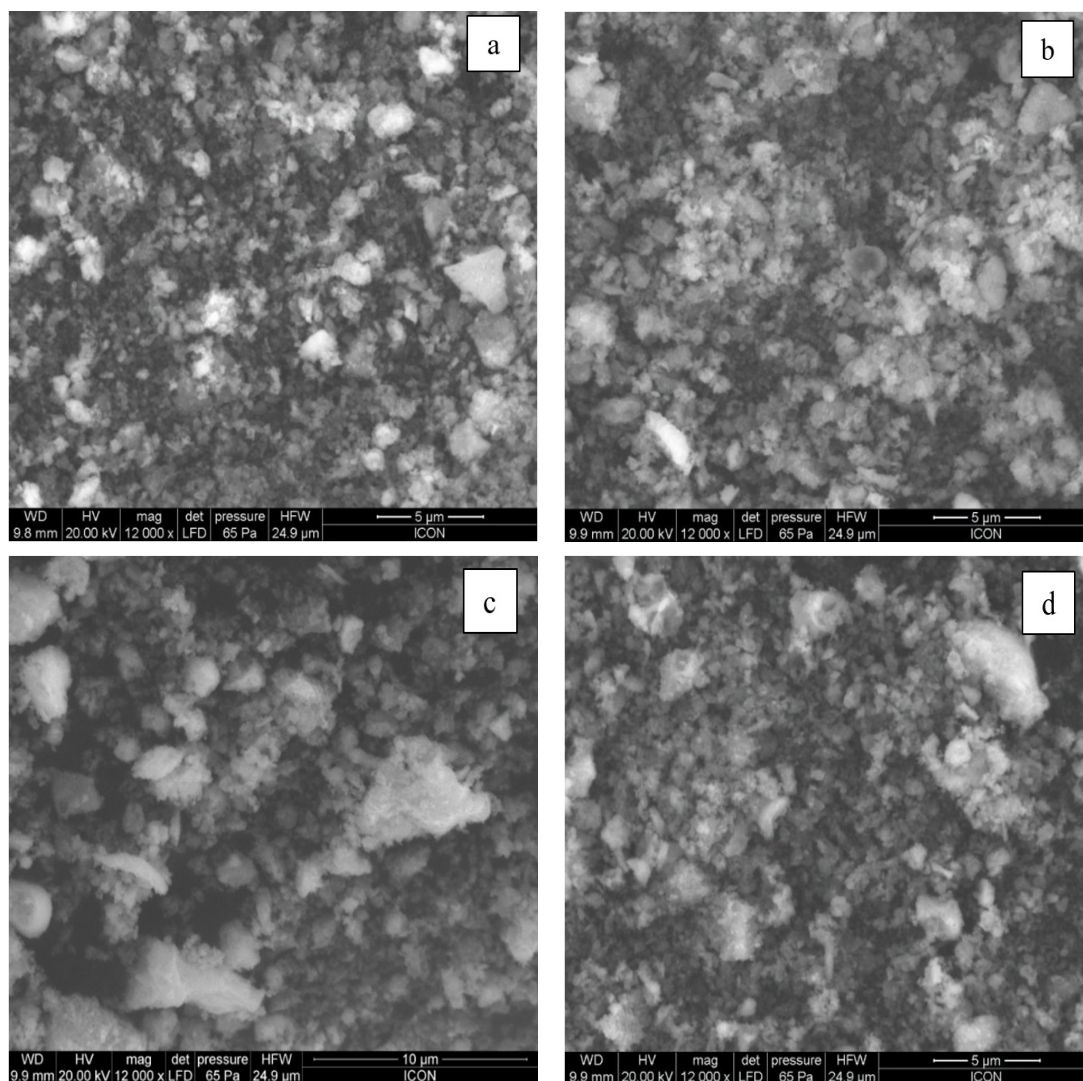


FIG. 5. SEM images of synthesized NdVO_4 nanoparticles sintered at $800\text{ }^\circ\text{C}$ for 4 hrs

3.5. EDX analysis

The composition of the synthesized nanoparticles was analyzed by investigating the Energy Dispersive X-ray Spectroscopy (EDX) as shown in Fig. 6. The sharp peaks corresponds to Nd, V, O elements without impurity and the composition approaches the right stoichiometry of NdVO_4 .

3.6. TEM analysis

To get a better understanding of the morphology of NdVO_4 TEM images were taken (Fig. 7(a, b, c, d)). It indicates the presence of NdVO_4 with size $45 - 90\text{ nm}$ which form bead type of aggregation throughout the region, on the contrary the image shows distinct nanoparticles of nearly spherical structure which are correlated well with the XRD results. SAED pattern also shows the spot type pattern which is indicative of the presence of single crystallite particles. No evidence was found for more than one pattern, suggesting the single phase crystalline nature of the material.

3.7. UV-Visible spectrum analysis

UV-Visible spectrum shows (Fig. 8) strong absorption peaks at $280, 593, \text{ and } 753\text{ nm}$ as shown in Fig. 8 the peak at 280 nm originates from ultraviolet (UV) absorption of VO_4^{3-} ions of NdVO_4 nanoparticles while a peak at 593 nm can be attributed to the Nd^{3+} transition of NdVO_4 nanoparticles. Extrapolating absorption edge would give band gap energy for NdVO_4 nanoparticles which is 3.50 eV . Due to wide band gap NdVO_4 is a UV active material.

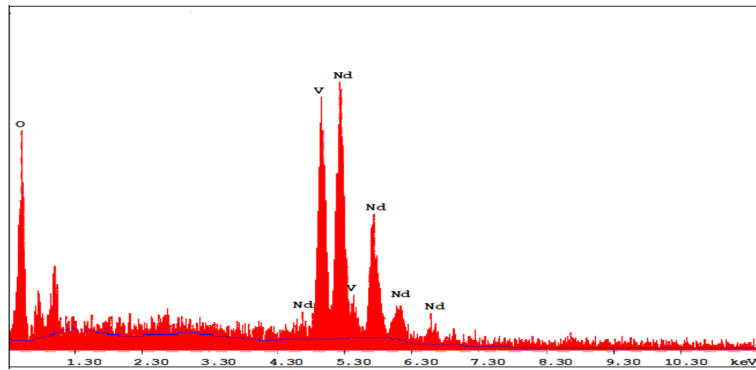


FIG. 6. EDX pattern synthesized NdVO_4 nanoparticles sintered 800°C for 4 hrs

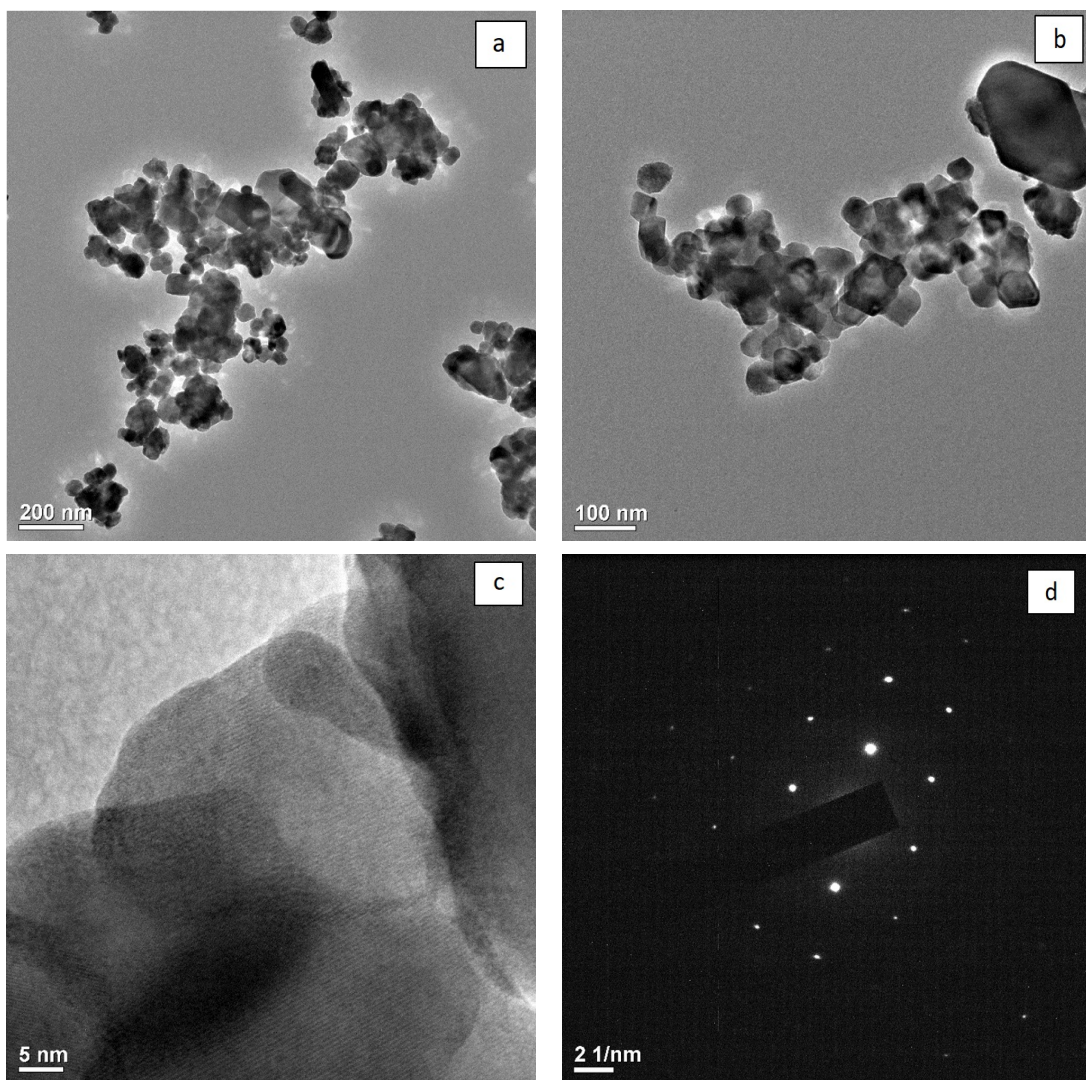
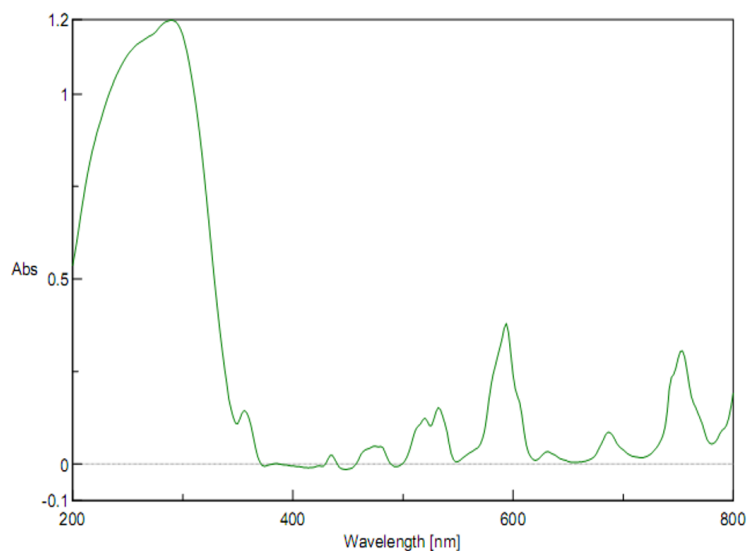


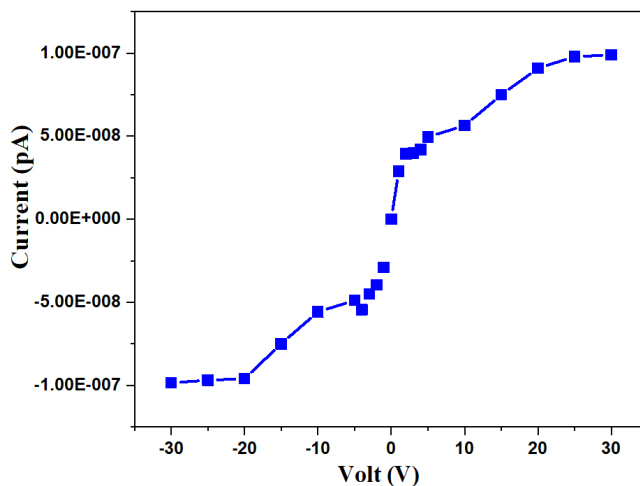
FIG. 7. TEM image with SAED pattern of synthesized NdVO_4 nanoparticles

FIG. 8. UV-Visible spectrum (DRS) of NdVO_4 nanoparticles

4. Electrical properties of sensor

4.1. I–V characteristics

Figure 9 depicts I–V characteristics of NdVO_4 films. It is clear from the symmetrical I–V characteristics that the silver contacts on the films were ohmic in nature. The voltage applied was in the range 1 – 30 V.

FIG. 9. I–V characteristics of the NdVO_4 film

4.2. Electrical conductivity

Figure 10 shows variation of conductivity with temperature. Conductivity values of the sample increases with operating temperature. The increase in conductivity with an increase in temperature is attributed to the semiconducting nature of NdVO_4 nanoparticles. It is observed from the Fig. 10 that electrical conductivities of the NdVO_4 thick film samples increases with an increase in the temperature range from 25 to 350 °C in air ambient.

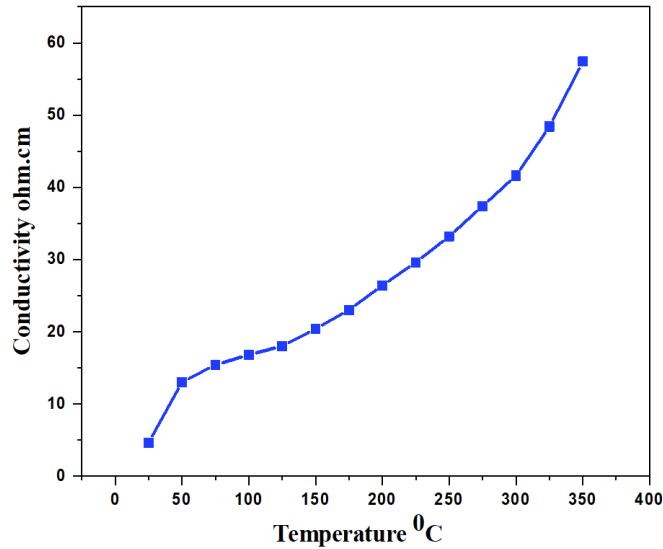


FIG. 10. Conductivity-temperature profiles of NdVO₄

5. Sensing performance of sensor

5.1. Gas response, selectivity, response and recovery time

The relative response (S) to a target gas is defined as the ratio of the change in conductance of a sample upon exposure of the gas to the original conductance in air, which can be calculated by following equation:

$$S = \frac{G_g - G_a}{G_a},$$

where G_a – conductance in air and G_g – conductance in a sample gas.

Specificity or selectivity is defined as the ability of a sensor to respond to a certain gas in the presence of different gases. Response time (RST) is defined as the time requires for a sensor to attain 90 % of the maximum increases in conductance on exposure to the target gas.

Recovery time (RCT) is the time taken to get back 90 % of the original conductance in air.

5.2. Sensing performance of NdVO₄ thick films. Response of sensors to various gases

The response of NdVO₄ sample variation for different gases with operating temperature is represented in Fig. 11. It is clear from the figure that the gas responses goes on increasing and attain to their respective maxima and decreased further with increase in operating temperatures. It is clear from the figure that the NdVO₄ shows the largest response to LPG at 275 °C.

5.3. LPG gas response and gas concentration

Figure 12 represents the variation of LPG response with NdVO₄ thick film sensor. For NdVO₄ thick films the response values were observed to increase continuously with increasing gas concentration up to 1000 ppm at 275 °C. The rate of increase in response was up to 1000 ppm continuously. But there is larger increase in response from 300 to 600 ppm.

5.4. Selectivity factor of NdVO₄ for various gases

Figure 13 depicts the selectivity of NdVO₄ thick film to 1000 ppm of LPG gas against various gases at 275 °C. It is clear from the Fig. 13. That NdVO₄ sensor shows not only enhanced response towards LPG but also high selectivity.

5.5. Response and recovery time

The response and recovery of NdVO₄ sensor are the response was quick (~ 13 s) to 1000 ppm of LPG, while the recovery was fast (~ 15 s, Fig. 14). The quick response may be due to faster oxidation of gas. The negligible quantity of the surface reaction product and its high volatility explains its quick response and fast recovery to its initial chemical status.

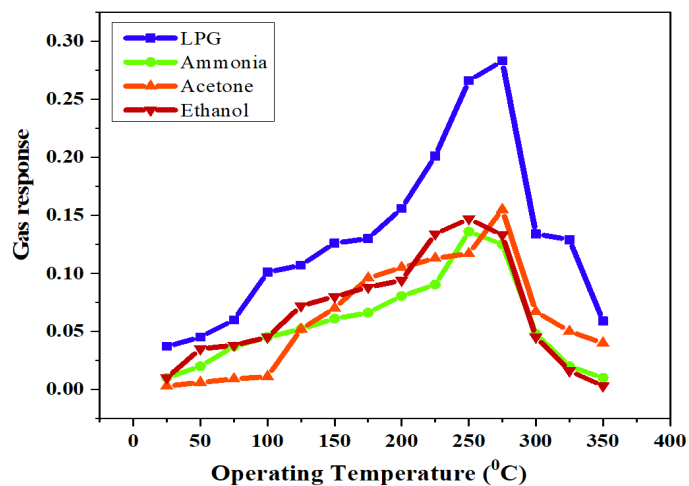


FIG. 11. Variation for different gas responses with operating temperatures

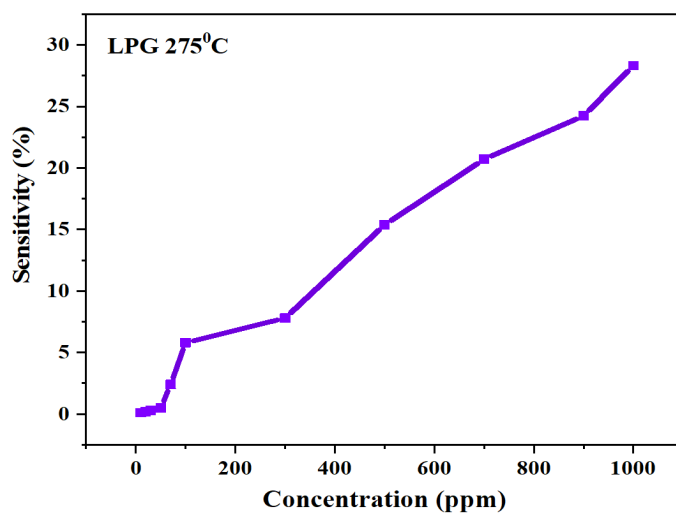


FIG. 12. Variation of gas response with gas concentration

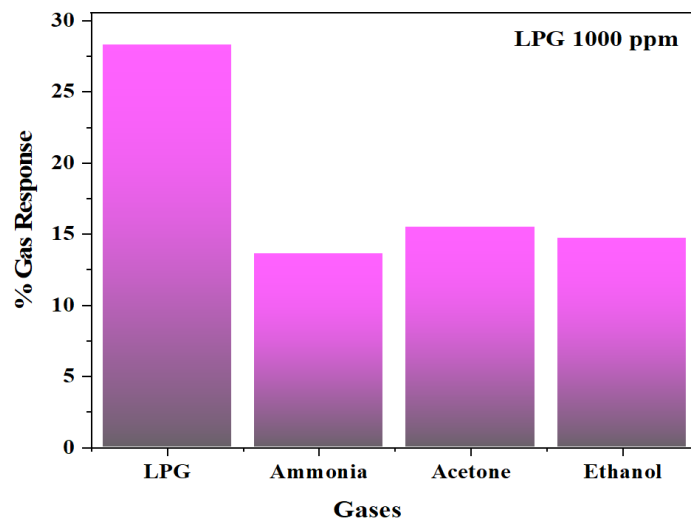


FIG. 13. Selectivity factor of sensor for various gases

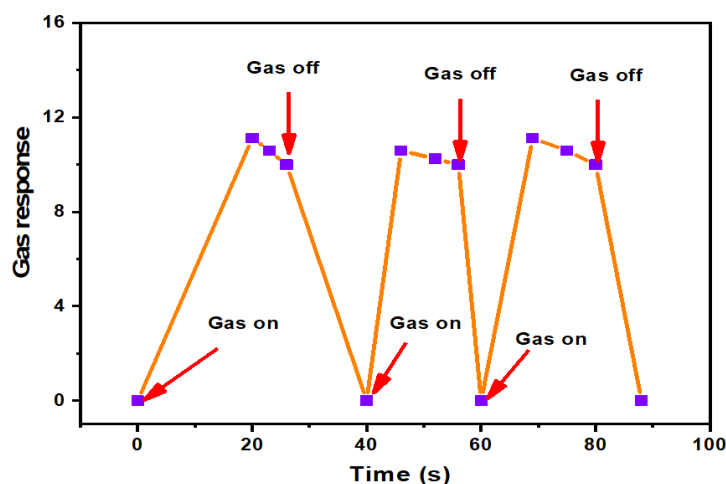
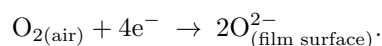


FIG. 14. Variation of gas response with gas concentration

6. Discussion

Gas sensing mechanism is generally explained in terms of conductance either by adsorption of atmospheric oxygen on the surface and/or by direct reaction of lattice oxygen or interstitial oxygen with the test gases. In case of former, the atmospheric oxygen adsorbs on the surface by extracting an electron from conduction band, in the form of super-oxide or peroxides, which are mainly responsible for the detection of the test gases. At higher temperature, the adsorbed oxygen captures the electrons from conduction band as:



It would result in decreasing conductivity of the film. When LPG reacts with the adsorbed oxygen on the surface of the film, it gets oxidized to CO_2 and H_2O by following series of intermediate stage. This liberates free electrons in the conduction band. The final reaction takes place as:



This shows n-type conduction mechanism. Thus generated electrons contribute to a sudden increase in conductance of the thick film. The NdVO_4 misfit regions dispersed on the surface would enhance the ability of base materials to absorb more oxygen species giving high resistance in air ambient. Therefore response was obtained to 1000 ppm LPG.

7. Conclusions

Nanocrystalline NdVO_4 has been synthesized by the self-combustion route. This synthetic route may be used for the synthesis of other metal oxide. Among all other additives tested, NdVO_4 is outstanding in promoting the LPG gas sensing mechanism. NdVO_4 was found to be optimum and showed the highest response to LPG gas at 275°C . The sensor showed very rapid response and recovery to LPG gas. Sensing mechanism of NdVO_4 was the substitution of lattice oxygen by LPG gas. The material gains electrons in this substitution. The sensor has good selectivity to LPG against, Acetone, Ethanol and NH_3 .

Acknowledgements

The authors are thankful to Honorable Principal Dr. V.M. Sarode and N.G. Vedak for providing necessary facilities during the research work. We are thankful to CIF Savitribai Phule Pune University, Shivaji University Kolhapur, BIT Bengaluru, SAIF IIT Powai and SAIF IIT Madras for providing the technical, instrumental and supports for this research work. We are also thankful to Nagesh Bhandri for his help during experimental work.

Conflict of interest

The authors declare no conflicts of interest.

References

- [1] Kohl D. Surface processes in the detection of reducing gases with SnO₂-based devices. *Sensors Actuators*, 1989, **18**, P. 71–113.
- [2] Bangale S.V., Prakshale R.D., Bamane S.R. Nanostructured CdFe₂O₄ Thick Film Resistors as Ethanol Gas Sensors. *Sensors & Transducers Journal*, 2012, **146** (11), P. 133–144.
- [3] Akiyama M., Yamazoe N. High-temperature potentiometric/amperometric NO_x sensors combining stabilized zirconia with mixed-metal oxide electrode. *Sensors Actuators B*, 1998, **13/14**, 619.
- [4] Bangale S.V., Patil D.R., Bamane S.R. Nanostructured spinel ZnFe₂O₄ for the detection of chlorine. *Sensors & Transducers Journal*, 2011, **134** (11), P. 107–119.
- [5] Bangale S.V., Patil D.R., Bamane S.R. Simple Synthesis of ZnCo₂O₄ Nanoparticles as Gas-sensing Materials. *Sensors & Transducers Journal*, 2011, **134** (11), P. 95–106.
- [6] Bangale S.V., Bamane S.R. Nanostructured MgFe₂O₄ Thick Film Resistors as Ethanol Gas Sensors Operable at Room Temperature. *Sensors & Transducers Journal*, 2012, **137** (2), P. 176–188.
- [7] Anand M. Study of tin oxide for hydrogen gas sensor applications. Thesis, University of South Florida, Graduate School, 2005, 98 p.
- [8] Aono H., Sato M., Traversa E., et al. Design of Ceramic Materials for Chemical Sensors: Effect of SmFeO₃ Processing on Surface and Electrical Properties. *J. Am. Ceram. Soc.*, 2001, **84**, P. 341–347.
- [9] Aono H., Traversa E., Sakamoto M., Sadaoka Y. Crystallographic characterization and NO₂ gas sensing property of LnFeO₃ prepared by thermal decomposition of Ln–Fe hexacyanocomplexes, Ln[Fe(CN)₆] \cdot *n*H₂O, Ln = La, Nd, Sm, Gd, and Dy. *Sens. Actuators B*, 2003, **94**, P. 132–139.
- [10] Das S., Chakraborty S., et al. Vanadium doped tin dioxide as a novel sulfur dioxide sensor. *Talanta*, 2008, **75**, P. 385–389.
- [11] Yu J.H., Choi G.M. Selective CO gas detection of CuO- and ZnO-doped SnO₂ gas sensor. *Sens. Actuators B*, 2001, **75**, P. 56–61.
- [12] Ansari Z.A., Ansari S.G., Ko T., Oh J.-H. Effect of MoO₃ doping and grain size on SnO₂-enhancement of sensitivity and selectivity for CO and H₂ gas sensing. *Sens. Actuators B*, 2002, **87**, P. 105–114.
- [13] Ivanovskaya M., Bogdanov P., et al. On the role of catalytic additives in gas-sensitivity of SnO₂-Mo based thin film sensors *Sens. Actuators B*, 2001, **77**, P. 268–274.
- [14] Bose S., Chakraborty S., et al. Methane sensitivity of Fe-doped SnO₂ thick films. *Sens. Actuators B*, 2005, **105**, P. 346–350.
- [15] Barsan N., Koziej D., Weimar U. Metal oxide-based gas sensor research: How to? *Sens. Actuators B*, 2007, **121**, P. 8–35.
- [16] Kamble D.R., Bangale S.V., Ghotekar S.K., Bamane S.R. Efficient Synthesis of CeVO₄ Nanoparticles Using Combustion Route and Their Antibacterial Activity. *J. Nanostruct.*, 2018, **8** (2), P. 144–151.
- [17] Yi Zhao, Mingwang Shao, et al. Hydrothermal synthesis of lanthanide orthovanadate: EuVO₄ particles and their fluorescence application. *Cryst.Eng.Comm.*, 2012, **14**, P. 8033–8036.
- [18] Tian Li, Chen Shan-min, et al. Effect of Eu³⁺-doping on morphology and fluorescent properties of neodymium vanadate nanorod-arrays. *Transactions of Nonferrous Metals Society of China*, 2020, **30**, P. 1031–1037.
- [19] Amarilla J.M., Casal B., Ruiz-Hitzky. Synthesis and characterization of the new mixed oxide NbVO₅. *Mater. Lett.*, 1989, **8**, 132.
- [20] Parag A., Deshpande P.A., Giridhar M. Photocatalytic degradation of dyes over combustion-synthesized Ce_{1-x}Fe_xVO₄. *Chemical Engineering Journal*, 2010, **185**, P. 571–577.
- [21] Suzuki H., Masuda Y., Miyamoto M. Magnetic and Specific Heat Studies of NdVO₄. *J. Phys. Soc. Jpn.*, 1983, **52**, 250.
- [22] Saji H., Yamadaya Y., Asanuma M. Magnetic Properties of RXO₄ System. *J. Phys. Soc. Jpn.*, 1970, **28**, 913.
- [23] Peng X.N., Zhang X., Yu I., Zhou I. Phase relations and optoelectronic characteristics in the NdVO₄–BiVO₄ system. *Mod. Phys. Lett. B*, 2013, **22**, 2647.
- [24] Bangale S.V., Prakshale R.D., et al. A New Hydrogen Sensor with Nanostructured Zinc Magnesium Oxide. *Sensors & Transducers Journal*, 2012, **137** (2), P. 176–188.
- [25] Khamkar K.A., Bangale S.V., et al. A Novel Combustion Route for the Preparation of Nanocrystalline LaAlO₃ Oxide Based Electronic Nose Sensitive to NH₃ at Room Temperature. *Sensors & Transducers Journal*, 2012, **146** (11), P. 145–155.
- [26] Mahapatra S., Madras T., Guru T.N. Row Kinetics of photoconversion of cyclohexane and benzene by LnVO₄ and LnMo_{0.15}V_{0.85}O₄ (Ln = Ce, Pr and Nd). *Ind. Eng. Chem. Res.*, 2007, **46**, 1013.
- [27] Amarilla J.M., Casal B., Ruiz-Hitzky E. Synthesis and characterization of the new mixed oxide NbVO₅. *Mater. Lett.*, 1989, **8**, P. 132–136.
- [28] Ekthammathat N., Thongtem T., Phuruangrat A., Thongtem S. Synthesis and Characterization of CeVO₄ by Microwave Radiation Method and Its Photocatalytic Activity. *J. Nanomater.*, 2013, **1**, 434197.